Molecular Chemical Structure on Poly(methyl methacrylate) (PMMA) Surface Studied by Sum Frequency Generation (SFG) Vibrational Spectroscopy

Jie Wang,[†] Chunyan Chen,[‡] Sarah M. Buck,[†] and Zhan Chen*[,†,‡]

Department of Chemistry, University of Michigan, Ann Arbor, Michigan 48109, and Department of Macromolecular Science and Engineering, University of Michigan, Ann Arbor, Michigan 48109

Received: August 17, 2001; In Final Form: September 21, 2001

The molecular chemical structure of poly(methyl methacrylate) (PMMA) surface has been studied by sum frequency generation (SFG) vibrational spectroscopy. By using various methods, we have shown that reflected SFG spectra of PMMA collected in our experiments only come from the polymer/air interface, not from the polymer/substrate or the bulk polymer. These SFG spectra are dominated by the vibrational bands from the ester methyl group. Ranges of orientation and orientation distribution of the ester methyl group on the PMMA surface have been deduced. The antisymmetric stretching vibrational band of the alpha methyl group has been detected on the PMMA surface. Analysis shows that the alpha methyl groups are lying down on the surface. The methylene group has not been observed in SFG spectra. For comparison, we have also studied surface chemical structures of poly(methyl acrylate) (PMA) and dimethyl succinate by SFG.

Introduction

Many of the chemical and mechanical properties of polymers, such as wettability, friction, lubricity, wearability, charge storage capacity, electrical response, and biocompatibility, are determined by their molecular surface structures, such as coverage and orientation of surface functional groups.[1−5] An extensive database of detailed correlations between surface properties and surface structure is necessary to facilitate the controlled design of polymers for specific uses. However, very little work has been reported on such structure−property correlations due to the lack of powerful analytical techniques that can probe molecular level polymer surface structure.

Poly(methyl methacrylate) (PMMA) is widely used as materials for biomedical implants, barriers, membranes, micro lithography, and optical applications.[2,6−9] In fact, it is the first implanted biomedical polymer which has been used since the 1950s.[2] In all these applications, understanding surface structures of PMMA is very important. PMMA surfaces have been extensively studied by many research groups by various techniques[10−18] including surface tension measurements, secondary ion mass spectrometry (SIMS), and X-ray photoelectron spectroscopy (XPS), but some molecular level details of surface structures of PMMA, such as orientations of different surface functional groups, are still unclear.

In recent years, SFG has become a very powerful and highly versatile spectroscopic tool for surface and interface studies, which not only permits identification of surface molecular species, but also provides information about surface structure, such as coverage and orientation of surface functional groups.[19−34] The SFG technique can be used to probe any surface or interface accessible by light and no vacuum is required. It has all the common advantages of optical techniques: it is nondestructive and is highly sensitive with good spatial, temporal and spectral resolution. In an SFG setup, a pulsed visible laser beam (frequency ω_{vis}) and a tunable pulsed IR beam (ω_{ir}) are overlapped spatially and temporally on a surface. The light emitted by the nonlinear process at the sum frequency, $\omega_{sum} = \omega_{vis} + \omega_{ir}$, is detected by a photodetector (Figure 1). The intensity of the light at ω_{sum} is proportional to the square of the sample's second-order nonlinear susceptibility, which vanishes when a material has inversion symmetry under the electric-dipole approximation. The majority of bulk materials possess inversion symmetry, therefore, they do not generate a sum frequency output; but surfaces which lack inversion symmetry do. Both theoretical calculations and experimental results show that SFG is submonolayer sensitive. A plot of SFG intensities vs the frequency of the IR laser produces the vibrational spectrum of the surface species. As SFG is a polarized light experiment, the orientation of surface molecules can also be deduced by using different polarization combinations of input and output beams.[21,32,33,35−38] The surface sensitivity of SFG on polymer materials has been demonstrated.[39,40] In this paper, we will study the molecular chemical structure of PMMA surface by SFG.

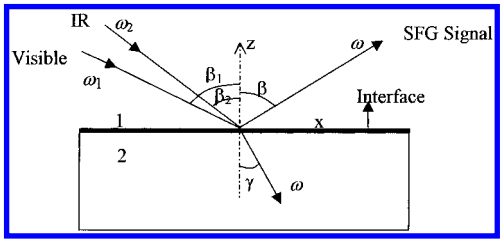

Figure 1. Schematic plot of the reflection SFG setup.

Experimental Methods

1. SFG. In our experiments, sum frequency spectra were collected by overlapping a visible and a tunable IR beam on a polymer surface, at incident angles of 60° and 54° (versus the surface normal), respectively (Figure 1). The visible beam at 532 nm was generated by frequency-doubling the fundamental

* Author to whom all correspondence should be addressed. Fax: 734-647-4865. E-mail: zhanc@umich.edu.
[†] Department of Chemistry.
[‡] Department of Macromolecular Science and Engineering.

10.1021/jp013161d CCC: $20.00
Published on Web 11/01/2001

output pulses of 20 ps pulse width from an EKSPLA Nd:YAG laser. The IR beam, tunable from 1000 to 4300 cm^{-1}, was generated from an EKSPLA optical parametric generation/amplification and difference frequency system based on LBO and $AgGaS_2$ crystals. Both beams were focused on the sample with diameters of about 0.5 mm. The sum frequency signal from the polymer surface was collected by a photomultiplier tube and processed with a gated integrator. A separate photomultiplier was used to collect the bulk SFG signal from a ZnSe plate as a reference channel. Two photodiodes were used to monitor the input visible beam and IR beam powers by collecting the back reflections of these two beams from focus lenses. Therefore, SFG spectra from the sample surfaces can be normalized either by the reference signal from ZnSe, or by the powers of the input laser beams. Surface vibrational spectra were obtained by measuring the SFG signal as a function of the input IR frequency. The monochromator in front of each photomultiplier can be tuned automatically while scanning the IR frequency, thus SFG spectra with large frequency range can be collected without any manual adjustments. In this study, SFG spectra with different polarization combinations including ssp (s-polarized sum frequency output, s-polarized visible input, and p-polarized infrared input), ppp, pss, and sps were collected.

The sample stage was manually adjusted to optimize the alignment. It can also be moved or rotated automatically in the X−Y plane by three computer-driven step motors. The moving step can be controlled as accurately as 5 μm or 1°. We can monitor the chemical homogeneity of the sample surface by mapping the surface SFG signals while continuously tuning the step motors. In our experiments, we observed that our sample surfaces were quite homogeneous.

2. Sample Preparation. PMMA (MW = 35 000) and poly(methyl acrylate) (PMA) (MW = 40 000) were purchased from Scientific Polymer Products, Inc., and used as received. Polymer films were prepared either by spin coating (for thin films) or solvent casting (for thick films). A spin coater from Specialty Coating Systems was used to spin coat 2 wt % polymer/toluene solution at 3000 rpm on fused silica (1 in. diameter and 1/8 in. thickness, from ESCO Products) to make thin polymer films. Thick polymer films were prepared by solvent casting the same solution on the same kind of substrate. All the polymer films were annealed at 80 °C for 12 h.

Theories for Analyzing SFG Spectra

1. Methods To Fit SFG Spectra. The SFG output intensity in the reflected direction can be written as[35]

$$I(\omega) = \frac{8\pi^3\omega^2 \sec^2\beta}{c^3 n_1(\omega)\, n_1(\omega_1)\, n_1(\omega_2)} |\chi^{(2)}_{\text{eff}}|^2 I_1(\omega_1)\, I_2(\omega_2) \qquad (1)$$

where $n_i(\omega)$ is the refractive index of medium i at frequency ω, β is the reflection angle of the sum frequency field, $I_1(\omega_1)$ and $I_2(\omega_2)$ are the intensities of the two input fields. $\chi^{(2)}_{\text{eff}}$ is the effective second-order nonlinear susceptibility tensor of the surface, which is related to the second-order nonlinear susceptibility $\chi^{(2)}$ in the lab coordinate system. Therefore, different tensor components of $\chi^{(2)}$ can be deduced from different components of $\chi^{(2)}_{\text{eff}}$ through measuring SFG spectra using different polarization combinations of the input and output beams:[35]

$$\chi^{(2)}_{\text{eff,ssp}} = L_{yy}(\omega)\, L_{yy}(\omega_1)\, L_{zz}(\omega_2) \sin\beta_2 \chi_{yyz}$$

$$\chi^{(2)}_{\text{eff,sps}} = L_{yy}(\omega)\, L_{zz}(\omega_1)\, L_{yy}(\omega_2) \sin\beta_1 \chi_{yzy}$$

$$\chi^{(2)}_{\text{eff,pss}} = L_{zz}(\omega)\, L_{yy}(\omega_1)\, L_{yy}(\omega_2) \sin\beta \chi_{zyy}$$

$$\begin{aligned}\chi^{(2)}_{\text{eff,ppp}} = &- L_{xx}(\omega)\, L_{xx}(\omega_1)\, L_{zz}(\omega_2) \cos\beta \cos\beta_1 \sin\beta_2 \chi_{xxz} \\ &- L_{xx}(\omega)\, L_{zz}(\omega_1)\, L_{xx}(\omega_2) \cos\beta \sin\beta_1 \cos\beta_2 \chi_{xzx} \\ &+ L_{zz}(\omega)\, L_{xx}(\omega_1)\, L_{xx}(\omega_2) \sin\beta \cos\beta_1 \cos\beta_2 \chi_{zxx} \\ &+ L_{zz}(\omega)\, L_{zz}(\omega_1)\, L_{zz}(\omega_2) \sin\beta \sin\beta_1 \sin\beta_2 \chi_{zzz} \qquad (2)\end{aligned}$$

Here χ_{yyz}, χ_{yzy}, χ_{zyy}, χ_{xxz}, χ_{xzx}, χ_{zxx}, and χ_{zzz} are different components of $\chi^{(2)}$ with the lab coordinates chosen such that z is along the interface normal and x is in the incident plane. $\chi^{(2)}_{\text{eff,ssp}}$, $\chi^{(2)}_{\text{eff,sps}}$, $\chi^{(2)}_{\text{eff,pss}}$, and $\chi^{(2)}_{\text{eff,ppp}}$ are components of the effective second-order nonlinear susceptibility measured in the experiment. For example, $\chi^{(2)}_{\text{eff,ssp}}$ means the element obtained by s-polarized sum frequency beam, s-polarized visible beam, and p-polarized IR beam. β, β_1, and β_2 are angles between the surface normal and the sum frequency beam, input visible beam, and the input IR beam, respectively (see Figure 1). L_{ii} ($i = x$, y, or z) are the Fresnel coefficients.

With IR−visible SFG, if the IR frequency is near vibrational resonance, $\chi^{(2)}_{\text{eff}}$ can be written as

$$\chi^{(2)}_{\text{eff}} = \chi_{\text{nr}} + \sum_q \frac{A_q}{\omega_2 - \omega_q + i\Gamma_q} \qquad (3)$$

χ_{nr} arises from the nonresonant background contribution, and A_q, ω_q, and Γ_q are the strength, resonant frequency, and damping coefficient of the vibrational mode q. Therefore, A_q, ω_q, and Γ_q can be obtained by fitting the SFG spectra.

2. Methods To Calculate the Orientation of Surface Functional Groups. Orientation of surface functional groups such as methyl or methylene can be determined by their ssp, sps, and ppp SFG spectra. Different components of $\chi^{(2)}$ are related to the respective components of the molecular hyperpolarizability (in the molecular coordinate system, which is a product of IR and Raman transition moments) by the average orientational angle of the functional group. Therefore, we can deduce the orientation information of each functional group after determining the corresponding components of $\chi^{(2)}$ by fitting SFG spectra and knowing the molecular hyperpolarizability.

Methyl groups have been treated as having C_{3v} symmetry in many cases, even though sometimes the real symmetry is lower.[21,36,37] In this paper, we will treat both the ester methyl group and the alpha methyl group as having C_{3v} symmetry. We will validate this assumption in a later discussion. We will also treat the methylene group as having C_{2v} symmetry, as in many published papers.

There are only two nonvanishing independent elements in the methyl symmetric stretch hyperpolarizability tensor, α_{ccc} and $\alpha_{aac} = \alpha_{bbc}$. For the antisymmetric stretch of the methyl group, ssp, sps, and ppp SFG spectra depend on one independent hyperpolarizability tensor element: α_{caa}.[35] For the methylene group, the only two nonzero independent components of the symmetric stretch are related by[37] $\alpha_{aac} = r\alpha_{ccc}$. Similar to the methyl group, SFG spectra of the antisymmetric stretching mode of the methylene group only depends on α_{caa}.

We can use Euler angles to specify the orientation of the molecular (abc) system with respect to the lab (xyz) system as depicted in Figure 2. In the case of an azimuthally isotropic

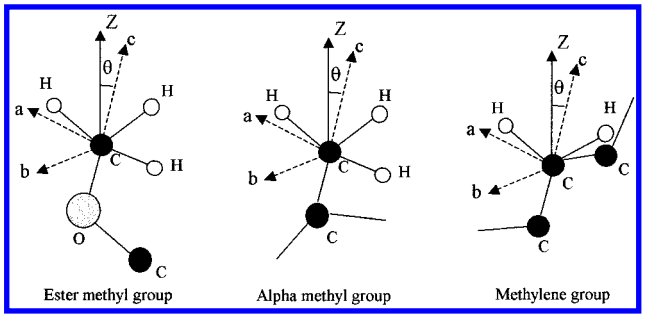

Figure 2. Orientation angle between surface normal and ester methyl, alpha methyl, and methylene groups: for methyl group, axis *c* is the principal axis of the methyl group. The *ab* plane is perpendicular to axis *c*. The *ac* plane contains one C−H bond. For the methylene group, axis *c* is the principal axis of the methylene group. The *ab* plane is perpendicular to axis *c*. The *ac* plane contains both C−H bonds.

interface, there are only four independent nonvanishing components for the second nonlinear susceptibility,[21] which are

$$\chi_{xxz} = \chi_{yyz}, \chi_{xzx} = \chi_{yzy}, \chi_{zxx} = \chi_{zyy}, \chi_{zzz}$$

For a methyl group with C_{3v} symmetry, we can determine the relationship between different components of the second-order nonlinear susceptibility in the lab coordinate system and the molecular hyperpolarizability in the molecular coordinate system by assuming a δ-function distribution of θ.[35,38] Thus, for the symmetric stretch we have

$$\chi_{xxz,s} = \chi_{yyz,s} = \frac{1}{2}N_s\alpha_{ccc}[\cos\theta\,(1+r) - \cos^3\theta\,(1-r)]$$

$$\chi_{xzx,s} = \chi_{yzy,s} = \chi_{zxx,s} = \chi_{zyy,s} = \frac{1}{2}N_s\alpha_{ccc}[\cos\theta - \cos^3\theta](1-r)$$

$$\chi_{zzz,s} = N_s\alpha_{ccc}[r\cos\theta + \cos^3\theta\,(1-r)] \qquad (4)$$

Here, $\alpha_{aac} = r\alpha_{ccc}$. For the antisymmetric stretch of methyl group we have

$$\chi_{yyz,as} = \chi_{xxz,as} = -\frac{\alpha_{caa}}{2}N_s(\cos\theta - \cos^3\theta)$$

$$\chi_{zxx,as} = \chi_{zyy,as} = \chi_{yzy,as} = \chi_{xzx,as} = \frac{\alpha_{caa}}{2}N_s\cos^3\theta$$

$$\chi_{zzz,as} = \alpha_{caa}N_s(\cos\theta - \cos^3\theta) \qquad (5)$$

Relations for the symmetric stretch of the methylene group has been deduced.[38,41] For the antisymmetric stretch of the methylene group, we find that the relations are the same as those in eq 5.

Usually, surface functional groups do not have the same orientation angle, and the δ-function approximation is not accurate. The orientation angle can be modeled by a Gaussian distribution:[42,43] $f(\theta) = C\exp[-(\theta-\theta_0)^2/2\sigma^2]$, where C is a normalization constant and σ is the root-mean-square width. Therefore, we have: $\chi_{xyz} = \int\chi_{xyz}\,f(\theta)\sin\theta\,d\theta$.

Results and Discussion

1. Proof of SFG Spectra from Polymer/Air Interface. Before discussing the details of PMMA SFG spectra, we want to prove that all the SFG spectra we will study in this paper came from the polymer/air surface, and has no contribution from the polymer/substrate interface or the bulk polymer materials. We use four related experiments to illustrate this.

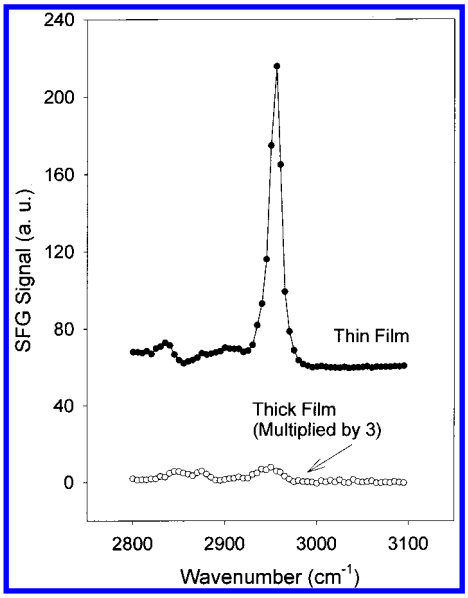

Figure 3. SFG spectra from the thin and thick PMMA films testing from the substrate side.

First, we collected the SFG spectra of thick (~200 μm) and thin (~100 nm) PMMA films and found that they were very similar. This shows that the SFG signal is not dominated by the contribution from the PMMA/substrate interface, otherwise the spectrum of the thin PMMA sample should be very different from that of the thick one. The IR beam would be absorbed by the thick film and would not reach the PMMA/substrate interface. This was proved by measuring the transmittance through the thick PMMA sample; almost no IR light was detected. The similar spectra for varying sample thicknesses also prove that the SFG spectra of PMMA are not dominated by the bulk signal, otherwise the SFG spectra from films with different thickness would be different.

We also tested both thin and thick film samples from the substrate side. Due to a change of Fresnel coefficients, the ssp signal from the thin film increases approximately 3 times when tested from the substrate side as opposed to the air side. At the same time, hardly any signal from the thick film was obtained (Figure 3, please note that the spectrum for the thick film shown in Figure 3 has been multiplied by three). As explained above, the IR laser was absorbed by the thick PMMA sample and could not reach the polymer/air interface. Therefore, we could not collect the SFG signal from the polymer/air interface by this experimental geometry. It also proves that the polymer/substrate interface and the bulk material of PMMA made no contribution to our SFG spectra. If that were the case, we would see a large signal from the thick PMMA sample with this experimental geometry.

The third experiment we used to demonstrate that SFG spectra came from the polymer/air interface was to test thin PMMA films from the substrate side, with samples in contact with water to remove the PMMA/air interface. The SFG signal intensity decreased substantially in comparison to the signal of the polymer/air interface detected from the substrate side.[44] This is another proof that reflected SFG signal is due to the PMMA/air interface.

Finally, we compared the reflected and transmitted SFG spectra of the thick PMMA film to detect bulk contributions. This method was first developed by Shen and co-workers.[39,45]

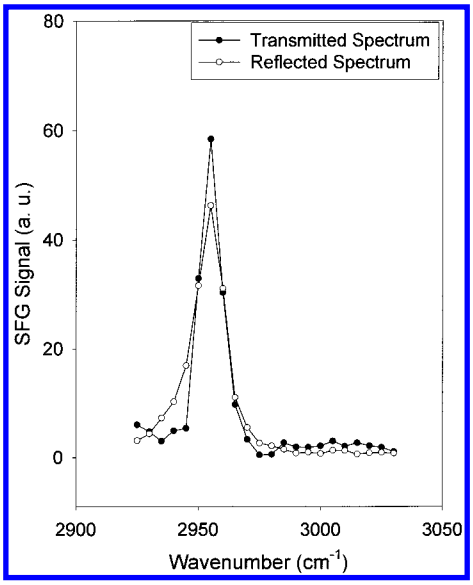

Figure 4. Reflected SFG spectrum and transmitted SFG spectrum of PMMA.

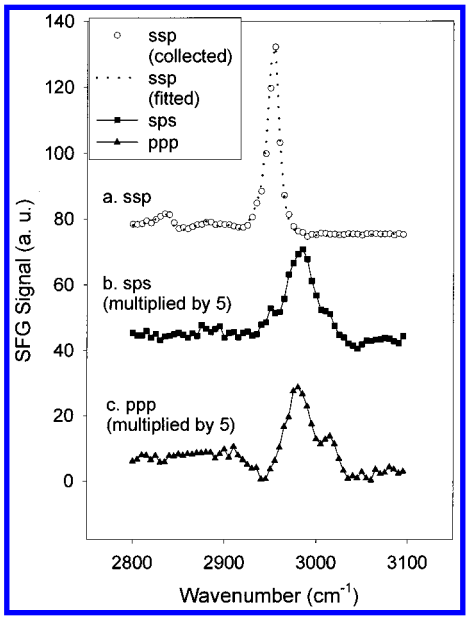

Figure 5. SFG spectra of PMMA: a. ssp; b. sps; c. ppp.

In our experiment, we found that the transmitted SFG spectrum was only slightly different from the reflected one in intensity (Figure 4). The coherent lengths of the two experimental geometries are very different.[39] At our test angle, the coherent length of the transmission geometry was over 1 order of magnitude larger than the reflection geometry. Therefore, the bulk contribution of the reflected SFG signal is small and can be ignored.

We have done similar experiments for PMA samples. As for PMMA, those SFG spectra are also dominated by the polymer/air interface.

2. SFG Spectra of PMMA. The PMMA SFG spectra collected by ssp, sps, and ppp polarization combinations in the reflection geometry are shown in Figure 5. The ssp spectrum in Figure 5a only has one dominant peak at 2955 cm^{-1}. By fitting the sps and ppp spectra in Figure 5b and Figure 5c, respectively, we find that in both spectra there are two major peaks at 2990 and 3016 cm^{-1}. We assigned these three peaks according to the studies on the bulk vibrational spectrum of PMMA published in the literature and by our own analysis.

TABLE 1: Assignment of FTIR and SFG Peaks for PMMA[a,b]

FTIR[48,49]			SFG	possible
CH_2	α-CH_3	O−CH_3	(this work)	assignment
		3025(as)	3016	(O)CH_3 (as)
	3000(as)	3002(as)	2990	(O)CH_3 (as), (C)CH_3(as)
2958(as)	2958(as)	2961(s)	2955	(O)CH_3 (s), (C)CH_3(as), CH_2(as)
2932(s)	2930(s)			

[a] as: antisymmetric stretch. [b] s: symmetric stretch.

The bulk vibrational spectrum of PMMA has been studied by various groups for decades.[46−49] The interpretation of these vibrational spectra is based on different methods, including comparison to the spectrum of methyl acetate, normal coordinate analysis, and selective deuteration of functional groups. The methylene C−H stretches are well documented as 2958 (antisymmetric) and 2933 (symmetric) cm^{-1}. Alpha methyl C−H stretches appear at 3000 cm^{-1} for the out-of-plane antisymmetric stretch, 2958 cm^{-1} for the in-plane antisymmetric stretch, and 2930 cm^{-1} for the in-plane symmetric stretch. According to the peak assignment in ref 49, the symmetric stretch peak of the ester methyl group is at 2961 cm^{-1}, two ester methyl antisymmetric stretches are at 3002 and 3025 cm^{-1}, respectively. The assignments of FTIR spectra (ref 48 for alpha methyl and methylene stretches, ref 49 for ester methyl stretches) and peaks observed in our SFG spectra and the possible assignments are summarized in Table 1. By using the methods we described above, we fit all the spectra in Figure 5 and the results are listed in Table 2.

As mentioned, we have observed three main peaks at 2955, 2990, and 3016 cm^{-1} in the SFG spectra of PMMA (Figure 5). The peak at 3016 cm^{-1} is from the antisymmetric stretching vibration of ester methyl group. The assignments of the other two peaks are more complicated. They may have more than one contributing vibrational mode. The peak at 2990 cm^{-1} may come from the antisymmetric stretch of the ester methyl group or alpha methyl group or both of them. The peak at 2955 cm^{-1} may be due to the symmetric stretch of the ester methyl group, antisymmetric stretch of the alpha methyl group, or antisymmetric stretch of the methylene group. It is also possibly due to the combination of these three modes. We will discuss the detailed assignments of these two peaks below.

First, we consider the peak at 2955 cm^{-1}. From formula 5, we found that for the antisymmetric stretch of the methyl group or the methylene group, we have: $\chi_{xzx} = \chi_{zxx}$, $\chi_{xxz} = \chi_{yyz}$, $\chi_{zzz} = -2\chi_{yyz}$. Also, in our experimental geometry,

$$L_{xx}(\omega)\, L_{zz}(\omega_1)\, L_{xx}(\omega_2) \cos\beta \sin\beta_1 \cos\beta_2 \approx L_{zz}(\omega)\, L_{xx}(\omega_1)\, L_{xx}(\omega_2) \sin\beta \cos\beta_1 \cos\beta_2$$

Substituting these formulas in eq 2 gives:

$$|\chi^{(2)}_{\mathrm{eff,ssp,as}}| = L_{yy}(\omega)\, L_{yy}(\omega_1)\, L_{zz}(\omega_2) \sin\beta_2 |\chi_{yyz,as}|$$

$$|\chi^{(2)}_{\mathrm{eff,ppp,as}}| = (L_{xx}(\omega)\, L_{xx}(\omega_1)\, L_{zz}(\omega_2) \cos\beta \cos\beta_1 \sin\beta_2 + 2L_{zz}(\omega)\, L_{zz}(\omega_1)\, L_{zz}(\omega_2) \sin\beta \sin\beta_1 \sin\beta_2) |\chi_{yyz,as}| \quad (6)$$

In our experiment, we can calculate that:

$$L_{yy}(\omega)\, L_{yy}(\omega_1)\, L_{zz}(\omega_2) \sin\beta_2 < (L_{xx}(\omega)\, L_{xx}(\omega_1)\, L_{zz}(\omega_2) \cos\beta \cos\beta_1 \sin\beta_2 + 2L_{zz}(\omega)\, L_{zz}(\omega_1)\, L_{zz}(\omega_2) \sin\beta \sin\beta_1 \sin\beta_2) \quad (7)$$

TABLE 2: Fitting Results for Figure 5

ω_q (cm^{-1})	Γ (cm^{-1})	A_{ssp}	A_{sps}	A_{ppp}	$A_{ppp,s}$ [a]	assignment
2840	7.0	0.37 ± 0.1				
2885	8.0	0.22 ± 0.1				
2910	8.0	0.15 ± 0.1		0.12 ± 0.1		
2935	8.0	-0.1 ± 0.1	0.0 ± 0.1	0.10 ± 0.1		
2955	5.0	1.52 ± 0.1	-0.08 ± 0.2	-0.17 ± 0.1	-0.44 ± 0.1	$(O)CH_3$ (s)
2990	10.5	0.0 ± 0.3	0.63 ± 0.1	0.64 ± 0.1	0.32 ± 0.1	$(O)CH_3$ (as), $(C)CH_3$(as)
3016	10.5	0.0 ± 0.3	0.46 ± 0.1	0.50 ± 0.1	0.30 ± 0.1	$(O)CH_3$ (as)

[a] $A_{ppp,s}$: fitting results for ppp spectra collected with smaller angles between the surface normal and input beams.

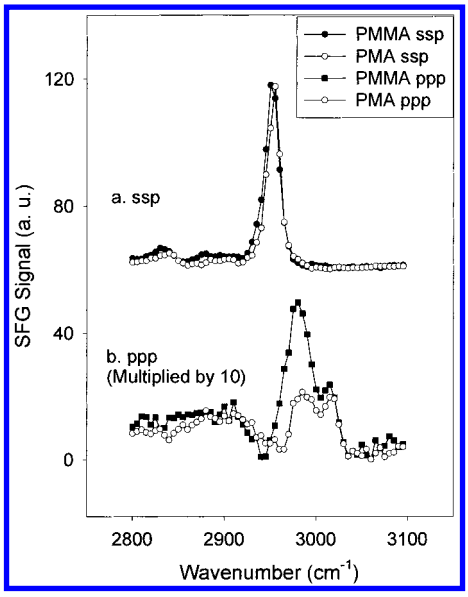

Figure 6. SFG spectra of PMA: a. ssp; b. ppp.

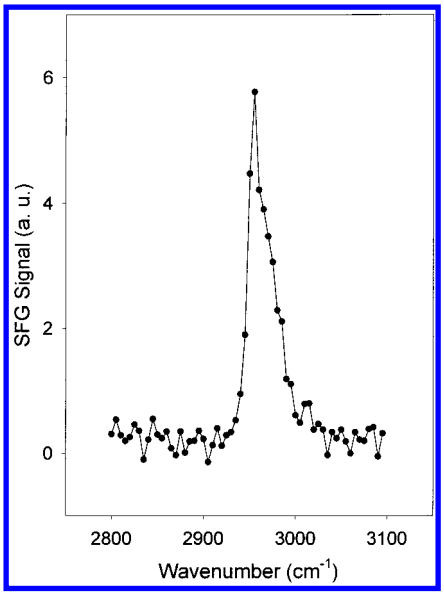

Figure 7. SFG spectrum (ppp) of PMMA collected by setup with smaller angles between the surface normal and input beams.

Using this relation, we can determine that the peak at 2955 cm^{-1} in our ssp SFG spectrum (Figure 5a) must be only from the symmetric stretch of the ester methyl group, containing almost no antisymmetric stretch signal from the alpha methyl or the methylene groups. Any signals from antisymmetric stretch in the ssp SFG spectrum should be stronger (due to the formula shown above) in the ppp spectrum. Instead the signal at 2955 cm^{-1} in the ppp SFG spectrum is very weak (Figure 5c), and the very strong peak at 2955 cm^{-1} in the ssp SFG spectra must come almost completely from the symmetric stretch of the ester methyl group.

We will prove that the peak at 2990 cm^{-1} comes from the antisymmetric stretch of the ester methyl and alpha methyl groups by comparison with the SFG spectrum of PMA. Figure 6 shows the ssp and ppp SFG spectra for PMA. The ssp spectrum of PMA (Figure 6a) is very similar to that of PMMA. There are two peaks, at 2990 and 3016 cm^{-1}, with similar intensities in the ppp spectrum of PMA (Figure 6b). Both peaks are due to the antisymmetric stretching modes of the ester methyl group. Comparing the PMA ppp spectrum to that of PMMA, we find that the peaks at 3016 cm^{-1} have similar intensities, but the PMMA peak at 2990 cm^{-1} has stronger intensity than that in PMA. We believe that two antisymmetric stretching peaks of ester methyl groups in PMMA should have similar intensity as in the PMA spectrum. Therefore, the strong 2990 cm^{-1} peak in PMMA must be due to both the asymmetric stretches of the ester methyl and the alpha methyl groups. Consequently, we can estimate the intensity contributed by the alpha methyl group for this peak.

3. Surface Chemical Structures of PMMA and PMA. As mentioned, various components of the second-order nonlinear susceptibility of the PMMA surface have been obtained by fitting SFG spectra in Figure 5. The fitting results are listed in Table 2. The refractive index of the interfacial layer on the PMMA surface n' is necessary for calculating some Fresnel coefficients to deduce the orientation of methyl and methylene groups. For example, $L_{zz}(\omega)$ can be written as

$$L_{zz}(\omega) = \frac{2n_2(\omega)\cos\beta}{n_1(\omega)\cos\gamma + n_2(\omega)\cos\beta}\left(\frac{n_1(\omega)}{n'(\omega)}\right)^2 \qquad (8)$$

where $n'(\omega)$ is the refractive index of the interfacial layer. Here, we developed a new experimental method to measure the refractive index (n') of the polymer interfacial layer.

From eqs 2 and 8 we know that ppp spectra are very sensitive to the value of n'. The refractive index n' should be very different from the two bulk media, air or polymer.[35] Recent experiments have shown that in order to match the calculated results from SFG spectra with the known orientation for hydrocarbon monolayers inferred from other experimental methods, the refraction index of the interfacial layer (n') should be close to 1.2.[35,50,51]

We measured n' by collecting PMMA ppp spectra while varying the angles of both the incident visible and IR beams vs the surface normal. As mentioned above, the angles between the surface normal and the visible and IR beams were usually 60° and 54°, respectively. We also collected ppp spectra with smaller angles between the surface normal and two input laser beams (visible: 46°, IR: 40°). The resulting SFG spectrum is shown in Figure 7. By calculating the ratio between the antisymmetric stretch signals in two ppp spectra collected with

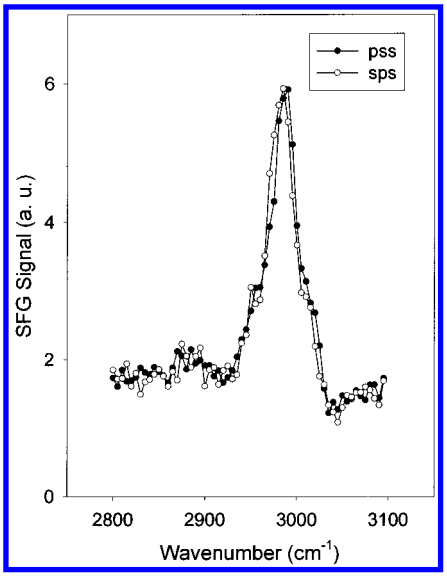

Figure 8. SFG spectrum (pss) of PMMA (To compare with the sps spectrum, the intensity was adjusted.).

different incident angles after normalizing other experimental parameters, we can deduce the value of n' to be 1.18 ± 0.05. We will use this number for our calculations at various frequencies. It is very close to the value published for a polymer monolayer on water.[35]

We have used the antisymmetric stretch of the ester methyl group at 3016 cm^{-1} to calculate the group's orientation, assuming C_{3v} symmetry for the group. The two antisymmetric peaks (2990 and 3016 cm^{-1}) have a splitting of about 30 cm^{-1} (Figure 5). Although the antisymmetric stretch of a methyl group with true C_{3v} symmetry should be degenerate, we assert the amount of error introduced by the assumption that the symmetry remains C_{3v} for PMMA ester methyl group is insignificant. According to Hirose et al.,[37] an assumption of C_{3v} symmetry for a spectrum with a 10 cm^{-1} splitting of two antisymmetric stretches of a methyl group introduces only 1% error in the calculations. By using a similar calculation, we found that with the 30 cm^{-1} splitting present in our spectra, the error introduced by the C_{3v} assumption is less than 5%. We find further evidence to validate the approximation of C_{3v} symmetry using the pss spectrum of PMMA. The pss and sps spectra should be very similar for methyl groups with C_{3v} symmetry. As can be seen in Figure 8, this is true for PMMA. Thus, we will use C_{3v} symmetry for the remainder of our calculations.

Equations 2 and 8 show that SFG spectra are not very sensitive to changes in the refractive index of the bulk polymer n_2. Calculations of the Fresnel coefficients vary only slightly (within 5%) for n_2 values ranging from 1.40 to 1.48. Therefore, we were able to ignore the frequency dependence of n_2, and used an intermediate value ($n_2 = 1.43$) for our calculation.

Using the n' deduced above (1.18 ± 0.05), we can calculate the ratio of $|\chi_{yyz,as}|/|\chi_{yzy,as}|$ for the antisymmetric stretch of the ester methyl group with various orientation angles. Figure 9 plots the relationship between $|\chi_{yyz,as}|/|\chi_{yzy,as}|$ and the orientation angle with the angle distribution σ. Here, the orientation angle is θ_0 in the formula of $f(\theta) = C \exp[-(\theta - \theta_0)^2/2\sigma^2]$. Since $f(\theta)$ sin θ is the real angle distribution rather than $f(\theta)$ after considering the azimuthal distribution, the real average orientation angle should be calculated by $\bar{\theta} = \int \theta\, f(\theta) \sin\theta\, d\theta$. However, we believe that θ_0 and σ can still be used to describe the average orientation angle and the angle distribution, thus we will continue to use them.

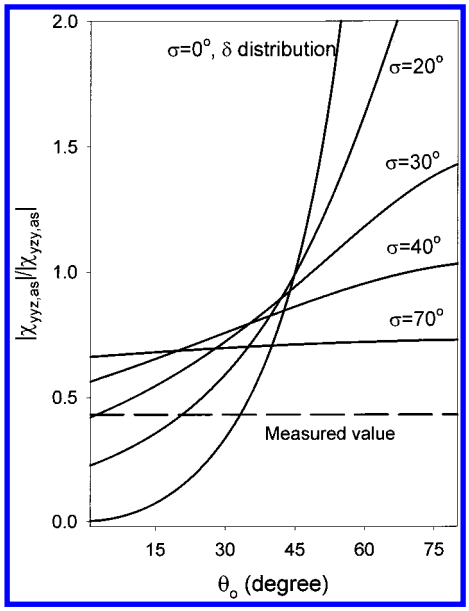

Figure 9. Relation between the $|\chi_{yyz,as}|/|\chi_{yzy,as}|$ and the orientation angle of the methyl group.

Figure 9 shows that there are multiple solutions for each value of $|\chi_{yyz,as}|/|\chi_{yzy,as}|$, thus it is impossible to identify the orientation angle θ_0 and angle distribution σ at the same time.[43] For example, if $|\chi_{yyz,as}|/|\chi_{yzy,as}|$ is measured to be 0.66, then among the many solutions are $\theta_0 = 0$ and $\sigma = 70°$ (a very broad angle distribution[43]) as well as $\theta_0 = 39°$ with a δ-angle distribution. Although we cannot determine the values of θ_0 and σ, we can obtain some information about them. The ratio of $|\chi_{yyz,as}|/|\chi_{yzy,as}|$ measured from the experiment is only 0.43. From Figure 9 we can see that the orientation angle θ_0 cannot be bigger than 33°, and the angle distribution σ is smaller than 31°. This indicates that the PMMA surface has some order, and the ester methyl groups on the surface are not very random. If we assume the angle distribution of the PMMA ester methyl groups to be a δ function, we deduce the orientation angle to be 33° from the surface normal. If we assume the average orientation angle to be 0° versus the surface normal, the angle distribution σ should be around 31°. The real structure of ester methyl groups on the PMMA surface should be between these two extremes.

The ratio of our measured $|\chi_{yyz,as}|/|\chi_{yzy,as}|$ (0.43) is not very different from the value of random distribution (0.66), suggesting experimental errors may significantly affect our measured results and by extension the deduced orientation information. Therefore, we also used absolute intensity of our SFG spectra to confirm the orientation information we acquired from the above calculation.[50]

We compared the calculated absolute intensity of ester methyl symmetric stretch in the ssp spectrum to the measured spectral intensity calibrated by using known standard z-cut quartz. To calculate the SFG intensity, the hyperpolarizability tensor component α_{ccc} and r (the ratio of the hyperpolarizability components α_{aac} and α_{ccc}) for the symmetric stretch of ester methyl groups should be available. The hyperpolarizability is the product of the IR dipole derivative and the Raman polarizability derivative. We used the value of the dipole derivative for the symmetric stretch of the ester methyl group in methyl acetate deduced from the normal mode calculation.[52] The value is 3.7×10^{-20} C, higher than the dipole derivative for the normal methyl group (2.9×10^{-20} C). Research shows that the Raman polarizability derivatives for symmetric stretches of different methyl groups are very similar; we will approximate

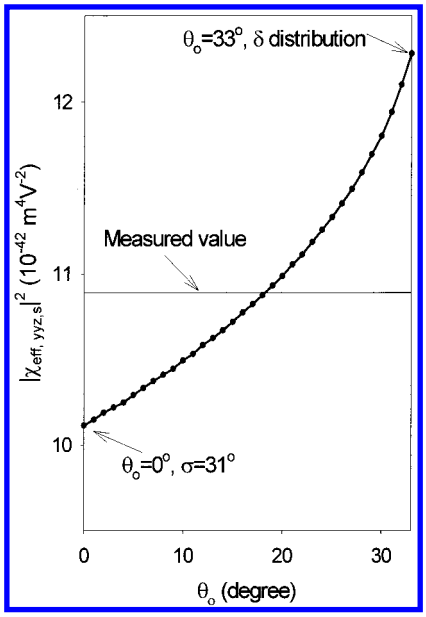

Figure 10. SFG (ssp) intensity of symmetric stretch of ester methyl groups on PMMA surface as a function of the possible orientation angle θ_0 (with the possible angle distribution σ) deduced from Figure 9.

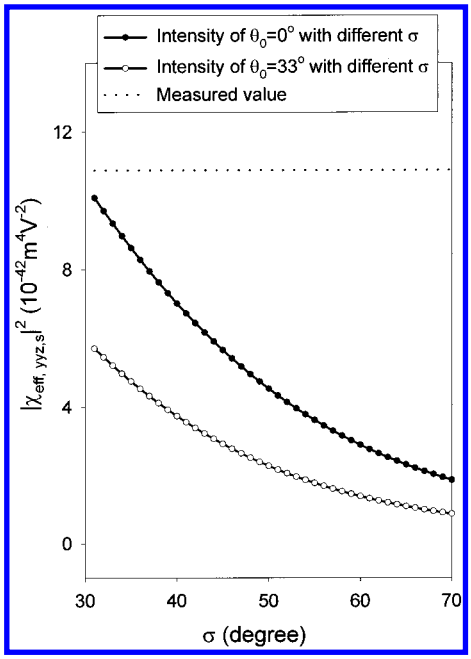

Figure 11. SFG (ssp) intensity of symmetric stretch of ester methyl groups on PMMA surface as a function of the angle distribution ($\sigma >$ 30°) of $\theta_0 = 0°$ and $\theta_0 = 33°$.

it to be 3.0×10^{-30} mC V^{-1} for our calculations.[53−55] From the intensity ratio of symmetric stretching bands of the ester methyl group in the ssp and ppp spectra, we calculated r (the ratio of the hyperpolarizability components α_{aac} and α_{ccc}) to be about 1.8, which is in the reasonable range of 1.6 to 4.3 for the methyl group.[35]

Since all the PMMA SFG spectra are dominated by the ester methyl group, we can conclude that their surface coverage is much higher than other functional groups. The surface density of the ester methyl group is estimated to be 5.0×10^{14} cm^{-2} according to the structures of polyethylene as well as the structures of various kinds of self-assembled monolayers.[56−58] It is observed that the ester-terminated SAMs have same structures as methyl-terminated SAMs.[58]

Figure 10 shows the calculated ssp SFG intensity of symmetric stretch of ester methyl groups on PMMA surface as a function of the possible orientation angle θ_0 (with the possible angle distribution σ) deduced from Figure 9. The measured SFG intensity is also shown in Figure 10 and it is in the range between the two extremes of the angle distributions. Since we cannot measure the exact surface density of ester methyl groups, we will not quantify the orientation angle and its distribution. From Figure 10, however, we can conclude that the results from the absolute intensity match the results deduced from Figure 9, and ester methyl groups are not random distributed on the PMMA surface. This conclusion can be further confirmed by the SFG intensity calculated for θ_0 of 0° and θ_0 of 30° with angle distribution σ larger than 30° (Figure 11). We can see that the calculated intensities are much lower than the measured result and decrease quickly when σ is bigger than 31°.

To further substantiate our claims of an ordered PMMA surface, we also collected the SFG spectra of a liquid sample dimethyl succinate ($CH_3OOCCH_2CH_2COOCH_3$, purchased from Lancaster Synthesis). The SFG spectra were also dominated by the ester methyl groups, and the measured $|\chi_{yyz,as}|/|\chi_{yzy,as}|$ value of asymmetric stretch of ester methyl groups was slightly larger than that of PMMA. The absolute spectral intensity was lower (Figure 12). From the same calculation as for PMMA, we found that the orientation angle distribution σ of ester methyl groups

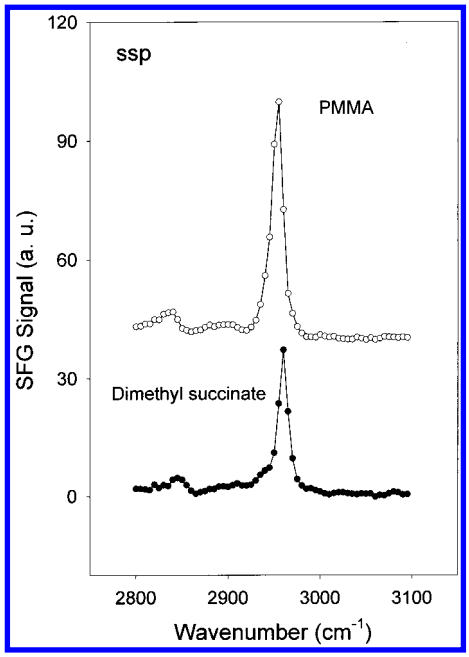

Figure 12. SFG (ssp) spectrum of dimethyl succinate.

on the surface of dimethyl succinate was much larger than that on the PMMA surface. This provides more proof that functional groups on PMMA surface have more orientational order than those of dimethyl succinate.

Figure 5b and 5c show the asymmetric stretch of the alpha methyl group of PMMA. There is no strong symmetric stretch signal of this group in the ssp spectra (Figure 5a), only weak signals in the wavenumber range 2800 cm^{-1} to 2930 cm^{-1}. This indicates that the alpha methyl groups tend to lie down on the surface plane. Our SFG experiments show that surface structures of PMMA and PMA are quite similar (Figure 6). Both surfaces are dominated by the ester methyl groups, and the signal of the alpha methyl group on the PMMA surface is quite weak. This explains the similarity of the surface tensions of PMMA[10,11] and PMA.[10]

Conclusion

SFG has been successfully applied to study the surface chemical structure of an important polymer, PMMA, at the molecular level. We have proved that SFG signal in our experiment only comes from the polymer/air interface, not from the polymer/substrate or the bulk polymer. The PMMA surface is dominated by the ester methyl groups. We have shown that the ester methyl groups on PMMA surface have some orientation orderings. From ssp, ppp, and sps SFG spectra, we deduce that the orientation and orientation distribution of ester methyl groups should be between the orientation angle of 33° vs the surface normal with a δ-angle distribution and 0° vs the surface normal with angle distribution σ of 31°. Comparison between the measured SFG intensity calibrated by a z-cut quartz and the calculated results confirms this conclusion. We also find that the alpha methyl groups tend to lie down on the PMMA surface, and the methylene groups are not detected on the PMMA surface. We have developed a new method to determine the refractive index of the interfacial layer of the polymer/air interface. For the PMMA/air interface, the refractive index of the interfacial layer has been measured by SFG to be 1.18 ± 0.05. The ratio of hyperpolarizability components α_{aac} and α_{ccc} of ester methyl symmetric stretch has been deduced to be about 1.8. For comparative purposes, we have also studied surface chemical structures of PMA and dimethyl succinate by SFG. The orientation of the ester methyl group on the PMA surface is similar to that on the PMMA surface, but the ester methyl groups are more random on the dimethyl succinate surface.

Acknowledgment. This work was supported by the start-up fund and the 2001 spring/summer research grant from the University of Michigan. We thank Dr. Jonas Kolenda and Dr. Zenonas Kuprionis from EKSPLA and Mr. Robert S. Tamosaitis from Altos for their helps in the installation of the SFG system.

References and Notes

(1) *Polymer Surface Dynamics*; Andrade, J. D., Ed.; Plenum Press: New York, 1988.
(2) Park, J. B.; Lakes, R. S. *Biomaterials: an Introducion*; Plenum Press: New York, 1992.
(3) Carbassi, F.; Morra, M.; Occhiellp, E. *Polymer Surfaces: From Physics to Technology*; John Wiley and Sons: Chichester, 1994.
(4) *Surface Modification of Polymeric Biomaterials*; Rataner, B. D., Castner, D. G., Eds.; Plenum Press: New York, 1996.
(5) *Polymer Surfaces and Interfaces II*; Feast, W. J., Munro, H. S., Richards, R. W., Eds.; John Wiley and Sons: New York, 1992.
(6) *Molecular Engineering of Ultrathin Films*; Stroeve, P., Franses, E. I., Eds.; Elsevier: London, 1987.
(7) *Langmuir−Blodgett Films*; Roberts, G. G., Ed.; Plenum Press: New York, 1990.
(8) Ulman, A. *An Introduction to Ultrathin Organic Films. From Langmuir−Blodgett to self-Assembly*; Academic Press: New York, 1991.
(9) Kuan, S. W.; Frank, C. W.; Lee, Y. H.; Eimori, T.; Allee, D. R.; Pease, R. F. W.; Browning, R. *J. Vac. Sci. Technol. B* **1989**, 7, 1745.
(10) Wu, S. *Polymer Interface and Adhesion*; Marcel Dekker: New York, 1982.
(11) Kwok, D. Y.; Leung, A.; Lam, C. N. C.; Li, A.; Wu, R.; Neumann, A. W. *J. Colloid Interface Sci.* **1998**, *206*, 44.
(12) Inoue, C.; Kaneda, Y.; Aida, M.; Endo, K. *Polym. J.* **1995**, *27*, 300.
(13) Cross, T.; Lippitz, A.; Unger, W.; Woll, C.; Hahner, G.; Braun, W. *Appl. Surf. Sci.* **1993**, *68*, 291.
(14) Leeson, A. M.; Alexander, M. R.; Short, R. D.; Briggs, D.; Hearn, M. J. *Surf. Interface Anal.* **1997**, *25*, 261.
(15) Briggs, D.; Fletcher, I. W.; Goncalves, N. M. *Surf. Interface Anal.* **2000**, *29*, 303.
(16) Leggett, G. J.; Vickerman, J. C. *Appl. Surf. Sci*. **1992**, *55*, 105.
(17) Deimel, M.; Rulle, H.; Liebing, V.; Benninghoven, A. *Appl. Surf. Sci*. **1998**, *134*, 271.
(18) Pignataro, B.; Fragalà, M. E.; Puglisi, O. *Nucl. Instrum. Methods Phys. Res. B* **1997**, *131*, 141.
(19) Shen, Y. R. *The Principles of Nonlinear Optics*; Wiley: New York, 1984.
(20) Shen, Y. R. *Annu. Rev. Phys. Chem.* **1989**, *40*, 327.
(21) Guyot-Sionnest, P.; Hunt, J. H.; Shen, Y. R. *Phys. Rev. Lett.* **1987**, *59*, 1597.
(22) Miranda, P. B.; Shen, Y. R. *J. Phys. Chem. B* **1999**, *103*, 3292.
(23) Bain, C. D. *J. Chem. Soc., Faraday Trans.* **1995**, *91*, 1281.
(24) Eisenthal, K. B. *Chem. Rev.* **1996**, *96*, 1343.
(25) Gragson, D. E.; Richmond, G. L. *J. Phys. Chem. B* **1998**, *102*, 3847.
(26) Walker, R. A.; Gruetzmacher, J. A.; Richmond, G. L. *J. Am. Chem. Soc.* **1998**, *120*, 6991.
(27) Chen, Z.; Gracias, D. H.; Somorjai, G. A. *Appl. Phys. B − Lasers and Optics* **1999**, *68*, 549.
(28) Gracias, D. H.; Chen, Z.; Shen, Y. R.; Somorjai, G. A. *Acc. Chem. Res.* **1999**, *320*, 930.
(29) Shultz, M. J.; Schnitzer, C.; Simonelli, D.; Baldelli, S. *Int. Rev. Phys. Chem.* **2000**, *19*, 123.
(30) Pizzolatto, R. L.; Yang, Y. J.; Wolf, L. K.; Messmer, M. C. *Anal. Chim. Acta* **1999**, *397*, 81.
(31) Kim, J.; Cremer, P. S. *J. Am. Chem. Soc.* **2000**, *122*, 12371.
(32) Briggman, K. A.; Stephenson, J. C.; Wallace, W. E.; Richter, L. J. *J. Phys. Chem. B* **2001**, *105*, 2785.
(33) Gautam, K. S.; Schwab, A. D.; Dhinojwala, A.; Zhang, D.; Dougai, S. M.; Yeganeh, M. S. *Phys. Rev. Lett.* **2000**, *85*, 3854.
(34) Löbau, J.; Wolfrum, K. *J. Opt. Soc. Am. B* **1997**, *14*, 2505.
(35) Zhuang, X.; Miranda, P. B.; Kim, D.; Shen, Y. R. *Phys. Rev. B* **1999**, *59*, 12633.
(36) Hirose, C.; Yamamoto, H.; Akamatsu, N.; Domen, K. *J. Phys. Chem.* **1993**, *97*, 10064.
(37) Hirose, C.; Akamatsu, N.; Domen, K. *J. Chem. Phys.* **1992**, *96*, 997.
(38) Hirose, C.; Akamatsu, N.; Domen, K. *Appl. Spectrosc.* **1992**, *46*, 1051.
(39) Wei, X.; Hong, S. C.; Lvovsky, A. I.; Held, H.; Shen, Y. R. *J. Phys. Chem. B* **2000**, *104*, 3349.
(40) Chen, Z.; Ward, R.; Tian, Y.; Baldelli, S.; Opdahl, A.; Shen, Y. R.; Somorjai, G. A. *J. Am. Chem. Soc.* **2000**, *122*, 10615.
(41) Duffy, D. C.; Davies, P. B.; Bain, C. D. *J. Phys. Chem.* **1995**, *99*, 15241.
(42) Wei, X.; Zhuang, X.; Hong, S. C.; Goto, T.; Shen, Y. R. *Phys. Rev. Lett.* **1999**, *82*, 4256.
(43) Simpson, G. J.; Rowlen, L. K. *J. Am. Chem. Soc.* **1999**, *121*, 2635.
(44) Wang, J.; Woodcock, S. E.; Buck, S. M.; Chen, C. Y.; Chen, Z. *J. Am. Chem. Soc.* **2001**, *123*, 9470.
(45) Shen, Y. R. *Appl. Phys. B* **1999**, *68*, 295.
(46) Dirlikov, S.; Koenig, J. L. *Appl. Spectrosc.* **1979**, *33*, 551.
(47) Dirlikov, S.; Koenig, J. L. *Appl. Spectrosc.* **1979**, *33*, 555.
(48) Lipschitz, I. *Polym.-Plast. Technol. Eng.* **1982**, *19*, 53.
(49) Dybal, J.; Krimm, S. *Macromolecules* **1990**, *23*, 1301.
(50) Wei, X.; Hong, S. C.; Zhuang, X.; Goto, T.; Shen, Y. R. *Phys. Rev. E* **2000**, *62*, 5160.
(51) Bell, G. R.; Bain, C. D.; Ward, R. N. *J. Chem. Soc., Faraday Trans.* **1996**, *92*, 515.
(52) Dybal, J.; Krimm, S. *J. Mol. Struct.* **1988**, *189*, 383.
(53) Galabov, B. S.; Dudev, T. *Vibrational Intensities*; Elsevier: Amsterdam, 1996.
(54) Steele, D.; Muller A. *J. Phys. Chem.* **1991**, *95*, 6163.
(55) Kats, S. M.; Vakhlyaeva, V. I.; Sverdlov, L. M. *Izy. Vyssh. Ucheb. Zaved.* **1969**, *12*, 125.
(56) Poirier, G. E. *Chem. Rev.* **1997**, *97*, 1117.
(57) Vallant, T.; Brunner, H.; Mayer, U.; Hoffmann, H.; Leitner, T.; Resch, R.; Friedbacher, G. *J. Phys. Chem. B* **1998**, *102*, 7190.
(58) Laibinis, P. E.; Bain, C. D.; Nuzzo, R. G.; Whitesides, G. M. *J. Phys. Chem.* **1995**, *99*, 7663.